analysis[14] yields the bounds $\gamma_{\max} \geq \gamma \geq \gamma_{\min}$ where, to first order in the small δ,

$$\gamma_{\max,\min} \approx \sqrt{\frac{I_3}{I_1} \cdot \frac{(I_2 - I_3) \pm 3\delta(1 + I_2/I_3)}{(I_1 - I_2) \mp 3\delta(1 + I_2/I_1)}} \tag{14}$$

Again, these quantities will be more sensitive if the moments of inertia are close than if they are widely spaced. For a vehicle with nominal inertias satisfying $I_1 = 2I_3$ and $I_2 = 1.5I_3$, and the 1% normalized inertia perturbations considered earlier, arctan γ can vary from 31.8 to 38.7 deg, a total range of 6.9 deg. Using Eqs. (13) and (14) together allows the possible variations in absolute separatrix directions to be quantified as a function of the inertia error bound δ, thus providing the desired insight into sizing δy as a function of δ.

Conclusions

This Note has derived a design procedure that prevents a spacecraft with a stuck-on thruster from experiencing a large net linear acceleration and, hence, a significant perturbation to its orbit. It was shown that such an acceleration is most likely to arise for a thruster that generates a torque that is nominally about the intermediate axis of an asymmetric vehicle, but that is in reality slightly offset from it. The simple technique that was developed to avoid this makes use of a small shift in thruster position. Expressions were derived to allow this shift to be sized to produce robust results despite small uncertainties in the geometry and mass properties of the vehicle.

Acknowledgments

This work was supported in part by the Automation, Robotics, and Simulation Division at NASA Johnson Space Center under Grant NAG9-874, with Technical Monitor Keith Grimm. The authors also wish to thank the Associate Editor and reviewer for many helpful suggestions.

References

[1] *Gemini Summary Conference*, NASA SP-138, Feb. 1967, pp. 52, 165.

[2] Hope, A. S., and Middour, J. W., "Clementine Mission Maneuver Performance and Navigation Control for the Spinning Phase," *Guidance and Control 1995*, Advances in the Astronautical Sciences, Vol. 88, Univelt, San Diego, 1995, pp. 463–476.

[3] *WIRE Mishap Investigation Board Report*, NASA, June 1999, pp. 14, 15.

[4] Leimanis, E., *The General Problem of the Motion of Coupled Rigid Bodies About a Fixed Point*, Springer-Verlag, Berlin, 1965, pp. 136–178.

[5] Chobotov, V. A., *Spacecraft Attitude Dynamics and Control*, Krieger, Malabar, FL, 1991, pp. 26–29.

[6] Randall, L. A., Longuski, J. M., and Beck, R. A., "Complex Analytic Solutions for a Spinning Rigid Body Subject to Constant Transverse Torques," *Astrodynamics 1995*, Advances in the Astronautical Sciences, Vol. 90, Pt. I, Univelt, San Diego, 1995, pp. 593–607.

[7] Tsiotras, P., and Longuski, J. M., "A Complex Analytic Solution for the Attitude Motion of a Near-Symmetric Rigid Body Under Body-Fixed Torques," *Celestial Mechanics and Dynamical Astronomy*, Vol. 51, No. 3, 1991, pp. 281–301.

[8] Williams, T. W., and Tanygin, S., "Dynamics of a Near-Symmetrical Spacecraft Driven by a Constant Thrust," *Proceedings of 6th AAS/AIAA Spaceflight Mechanics Meeting*, Advances in the Astronautical Sciences, Vol. 93, Pt. II, Univelt, San Diego, 1996, pp. 925–944.

[9] Livneh, R., and Wie, B., "New Results for an Asymmetric Rigid Body with Constant Body-Fixed Torques," *Journal of Guidance, Control, and Dynamics*, Vol. 20, No. 5, 1997, pp. 873–881.

[10] Williams, T. W., and Tanygin, S., "Dynamics of an Asymmetric Spacecraft Driven by a Constant Thrust: Perturbation Studies," *Proceedings of 7th AAS/AIAA Spaceflight Mechanics Meeting*, Advances in the Astronautical Sciences, Vol. 95, Pt. I, Univelt, San Diego, CA, 1997, pp. 211–229.

[11] Bracewell, B. N., and Garriott, O. K., "Rotation of Artificial Earth Satellites," *Nature*, Vol. 182, No. 4638, 1958, pp. 760–762.

[12] Kaplan, M. H., *Modern Spacecraft Dynamics and Control*, Wiley, New York, 1976, pp. 60, 61.

[13] Tanygin, S., "The General Problem of Attitude Motion," Ph.D. Dissertation, Dept. of Aerospace Engineering, Univ. of Cincinnati, Cincinnati, OH, Feb. 1999, pp. 14–19.

[14] Wilkinson, J. H., *The Algebraic Eigenvalue Problem*, Oxford Univ. Press, Oxford, England, U.K., 1965, pp. 69–75.

Experimental Robustness Study of Positive Position Feedback Control for Active Vibration Suppression

G. Song*
University of Akron, Akron, Ohio 44325-3903
and
S. P. Schmidt† and B. N. Agrawal‡
Naval Postgraduate School, Monterey, California 93943

I. Introduction

POSITIVE position feedback (PPF) control was introduced by Goh and Caughey in 1985 to control vibrations of large flexible space structures.[1] A PPF controller has several distinguished advantages as compared to then widely used velocity feedback control laws. It is insensitive to spillover,[2] where contributions from unmodeled modes affect the control of the modes of interest.[3,4] As a second-order low-pass filter, a PPF controller rolls off quickly at high frequencies and is well suited to controlling the lower modes of a structure with well separated modes.[3,5] Because of these advantages, PPF controller along with smart materials, in particular PZT (lead zirconate titanate) type of piezoelectric material, has been applied to many flexible systems to achieve active damping.[6–9] The design of a PPF controller requires the natural frequency of a structure. In practice, the structural natural frequency may not be known exactly or it may vary with time. When the frequency used in the PPF controller is different from that of the structure, the performance of the PPF control will adversely affected. Despite that PPF control is widely researched in literature, robustness study of PPF control when natural frequency is inexactly known is not reported. This motivates the authors to conduct experimental study of robustness of PPF control in active vibration suppression of a smart flexible structure.

II. PPF Control

PPF control requires that the sensor is collocated or nearly collocated with the actuator. In PPF control structural position information is fed to a compensator. The output of the compensator, magnified by a gain, is fed directly back to the structure. The equations describing PPF operation are given as

$$\ddot{\xi} + 2\zeta\omega\dot{\xi} + \omega^2\xi = G\omega^2\eta \tag{1}$$

$$\ddot{\eta} + 2\zeta_c\omega_c^2\dot{\eta} + \omega_c^2\eta = \omega_c^2\xi \tag{2}$$

where ξ is a modal coordinate describing displacement of the structure, ζ is the damping ratio of the structure, ω is the natural frequency of the structure, G is a feedback gain, η is the compensator coordinate, ζ_c is the compensator damping ratio, and ω_c is the frequency of the compensator. For the closed loop being stable, $0 < G < 1$ (Ref. 4).

To illustrate the operation of a PPF controller, assume a single degree-of-freedom vibration of the beam in the form of

$$\xi(t) = \alpha e^{i\omega t} \tag{3}$$

the output of the compensator at the steady state, provided the closed-loop system is stable, will be

$$\eta(t) = \beta e^{i(\omega t - \phi)} \tag{4}$$

Received 2 April 2001; revision received 30 July 2001; accepted for publication 7 September 2001.

*Assistant Professor, Department of Mechanical Engineering.
†Student, Department of Aeronautics and Astronautics.
‡Professor, Department of Aeronautics and Astronautics. Associate Fellow AIAA.

Report Documentation Page

Form Approved
OMB No. 0704-0188

1. REPORT DATE	2. REPORT TYPE	3. DATES COVERED
2001		**00-00-2001 to 00-00-2001**

4. TITLE AND SUBTITLE	5a. CONTRACT NUMBER
Experimental Robustness Study of Positive Position Feedback Control for Active Vibration Suppression	5b. GRANT NUMBER
	5c. PROGRAM ELEMENT NUMBER
6. AUTHOR(S)	5d. PROJECT NUMBER
	5e. TASK NUMBER
	5f. WORK UNIT NUMBER
7. PERFORMING ORGANIZATION NAME(S) AND ADDRESS(ES) **Naval Postgraduate School,Department of Aeronautics and Astronautics,Monterey,CA,93943**	8. PERFORMING ORGANIZATION REPORT NUMBER
9. SPONSORING/MONITORING AGENCY NAME(S) AND ADDRESS(ES)	10. SPONSOR/MONITOR'S ACRONYM(S)
	11. SPONSOR/MONITOR'S REPORT NUMBER(S)

12. DISTRIBUTION/AVAILABILITY STATEMENT
Approved for public release; distribution unlimited

13. SUPPLEMENTARY NOTES

14. ABSTRACT

15. SUBJECT TERMS

16. SECURITY CLASSIFICATION OF:			17. LIMITATION OF ABSTRACT	18. NUMBER OF PAGES	19a. NAME OF RESPONSIBLE PERSON
a. REPORT **unclassified**	b. ABSTRACT **unclassified**	c. THIS PAGE **unclassified**	**Same as Report (SAR)**	**4**	

In Eq. (4), the magnitude β is given as

$$\beta = \frac{A(\omega/\omega_c)}{\sqrt{\left(1-\omega^2/\omega_c^2\right)^2 + \left[2\zeta_c(\omega/\omega_c)\right]^2}}$$

where $A = \alpha(\omega_c/\omega)$.

In Eq. (4), the phase angle ϕ is given as

$$\phi = \tan^{-1}\left[\frac{2\zeta_c(\omega/\omega_c)}{1-\left(\omega^2/\omega_c^2\right)}\right] \tag{5}$$

When the structural modal frequency is much lower than the compensator natural frequency, the phase angle ϕ approaches zero according to Eq. (5). Substituting Eq. (4) with $\phi = 0$ into Eq. (1) results in

$$\ddot{\xi} + 2\zeta\omega\dot{\xi} + (\omega^2 - G\beta\omega^2)\xi = 0 \tag{6}$$

It is clear from Eq. (6) that the PPF compensator in this case results in the stiffness term being decreased, which is called *active flexibility*. When the compensator and the structure have the same natural frequency, it can be derived from Eq. (6) that the phase angle ϕ approaches $\pi/2$. Substituting Eq. (4) with $\phi = \pi/2$ into Eq. (1), the structural equation becomes

$$\ddot{\xi} + (2\zeta\omega + G\beta\omega)\dot{\xi} + \omega^2\xi = 0 \tag{7}$$

Equation (7) shows that the PPF compensator in this case results in an increase in the damping term, which is called *active damping*. When the structure frequency is much greater than that of the compensator, the phase angle ϕ approaches π. Substituting Eq. (4) with $\phi = \pi$ into Eq. (1) results in

$$\ddot{\xi} + 2\zeta\omega\dot{\xi} + (\omega^2 + G\beta\omega^2)\xi = 0 \tag{8}$$

It is clear that from Eq. (8) that the PPF compensator in this case results in an increase in the stiffness term, which is called *active stiffness*. To achieve maximum damping, ω_c should be closely matched to ω. Also, any structural natural mode below ω_c will experience increased flexibility.

The effect of the damping ratio ζ_c is discussed as follows. Larger values of the damping ratio ζ_c will result in a less steep slope thereby increasing the region of active damping. Figure 1 shows the bode plot for $\zeta_c = 0.5$ and for $\zeta_c = 0.1$. The difference in the slopes of the phase angle can be easily seen. A larger value of ζ_c ensures a larger region of active damping and therefore will increase the robustness of the compensator with respect to uncertain modal frequencies. However, it is expected to result in slightly less effective damping and result in increased flexibility at lower modes as a tradeoff.

III. Experimental Setup

A schematic of the equipment setup for vibration control using PPF is shown in Fig. 2. A cantilevered aluminum beam (its properties are shown in Table 1) is used as the object for vibration control. The beam has a PZT sensor and three PZT actuators. The PZT sensor actually consists of a pair of PZT patches, one on each side of the beam. Each PZT actuator also consists of a pair of PZT patches, one on each side of the beam. The PZT sensor can be considered nearly collocated with PZT actuator 1. Properties of the PZT are shown in Table 2. The aluminum beam is clamped such that its length was

Table 1 Cantilevered beam properties (aluminum beam type: 7075 T-6)

Quantity	Description	Value
t_b	Beam thickness	1.95 mm
w_b	Beam width	76.2 mm
L	Beam length	1.176 m
ρ_b	Beam density	2800 kg/m^3
E_b	Young's modulus	7.1×10^{10} N/m^2

Table 2 Properties of the piezoceramic actuators and sensor [Type: PZT-5A (Navy type II)]

Quantity	Description	Value
d_{31}	Lateral strain coefficient	1.8×10^{-10} Coul/N
E_p	Young's modulus	6.3×10^{10} N/m^2
ε_3^T	Absolute permittivity	1.5×10^{-8} Farad/m
ρ_p	PZT density	7.7×10^3 kg/m^3
t_p	PZT actuator and sensor thickness	0.5 mm
w_p	PZT actuator and sensor width	38.1 mm
L_a	Length of PZT actuators	63.5 mm
L_s	Length of PZT sensor	25.4 mm

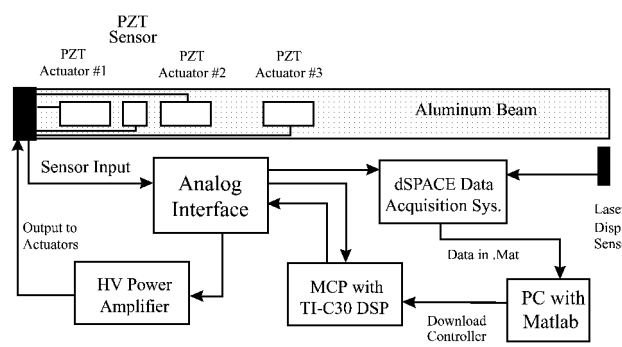

Fig. 2 Experimental setup schematic.

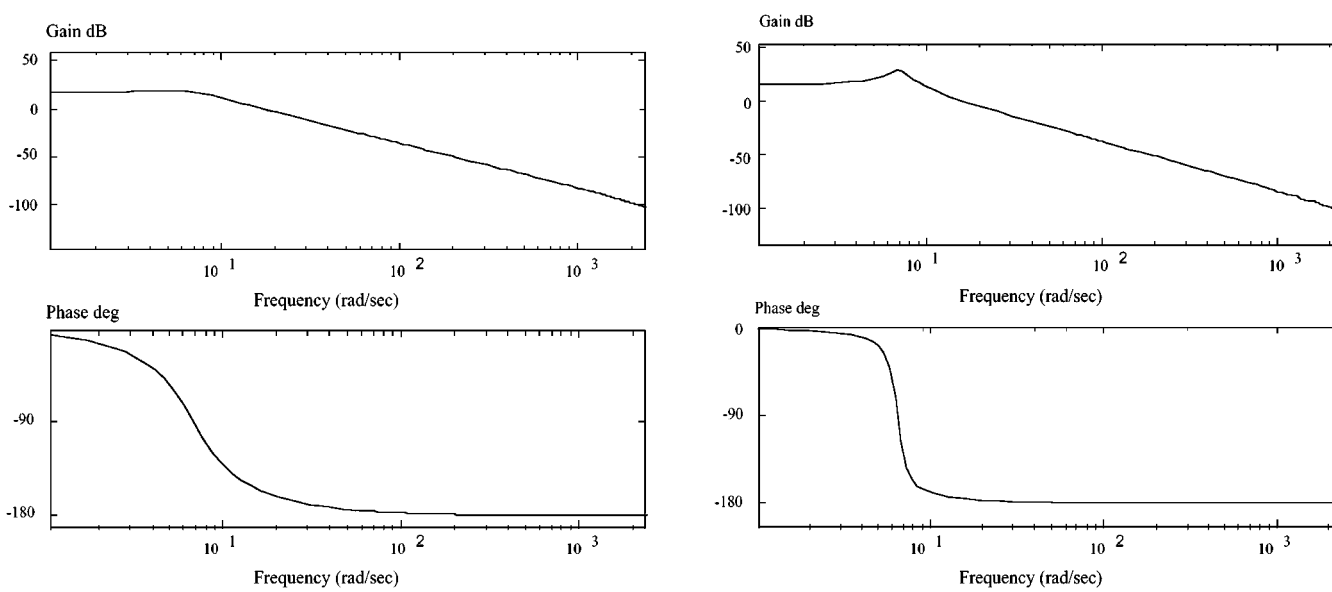

Fig. 1 Bode plot for PPF with $\zeta_c = 0.5$ (left) and $\zeta_c = 0.1$ (right).

parallel to the granite table below it. This allowed the bending to be strictly in the horizontal plane. A digital control system, called Modular Control Patch, is used to implement vibration suppression algorithms. It uses a TMS320C30 microprocessor. A digital data acquisition system using a TMS320C40 digital signal processor was used to record the experimental data.

IV. Experimental Procedure

Both open- and closed-loop tests were performed. All tests were started by manually exciting the beam. This was a simple and an effective method to excite the beam. For single-mode vibration suppression tests can be run with either all three actuator operational, or only the first actuator operational. For multimode suppression only the first PZT actuator was used. Because of modal shapes for the higher modes of the flexible beam, the second and the third actuators adversely impact damping of higher modes when the feedback strain information from the only PZT sensor is used. It is clear from Fig. 2 that the PZT sensor is not collocated or near collocated with these two actuators. For each test data were recorded for a time interval of 15 s after beam excitation. This allowed ample time to measure damping effects. The experimental data were then processed to show effectiveness of the tested control algorithm. A fast Fourier transform was performed to provide a power spectral density (PSD) plot of the beam response. PSD gives a measure of signal energy level at different frequencies. A comparison of the ratios of the last-second modal energy level in decibels to the initial one provides an indication of the damping effectiveness on this particular mode. Also, a direct comparison of the modal energy level drop with that of an open-loop response can indicate the effectiveness of the control algorithm.

Figure 3 shows the PSD plots for a multimode open-loop vibration. The solid line is for the first second of the 15-s test and the dashed line for the last second. A program was written to identify the modes excited and to compute the difference between the initial and final energy level in the decibel unit at the identified modal frequencies. The following data show energy level drops in decibels for the first four modes in the 15-s free vibration: first mode (1.33 Hz), 9.52 dB; second mode (7.1 Hz), 22.38 dB; third mode (19.0 Hz), 48.98 dB; fourth mode (38.2 Hz), 61.94 dB. It is clear that vibrations of the third and fourth modes quickly damp out. The first and second modes become the major concern for vibration suppression.

V. Experimental Robustness Study of PPF in Single Mode Vibration Suppression

One of the documented drawbacks of PPF is that its design requires the knowledge of modal frequency. If the targeted frequency is altered or is simply miscalculated, PPF damping would be severely affected. To test the robustness of PPF with respect to the modal frequency, experiments of PPF with inaccurate modal frequency from 25 to 400 % of the nominal value were conducted. Experiments with different value of ζ_c were also tested. Three values were used for ζ_c: 1, 0.5, and 0.25. This set of experiments was carried out to study the impact of compensator damping ratio on compensator robustness and on possible increased flexibility at lower modes. From the analysis in Sec. II, increasing the value of the damping ratio will provide a wider frequency range for active damping, but it is expected that its effectiveness at the target frequency will be reduced. In these experiments only PZT actuator one is used along with the PZT sensor. The PPF controller employs $G = 0.086$.

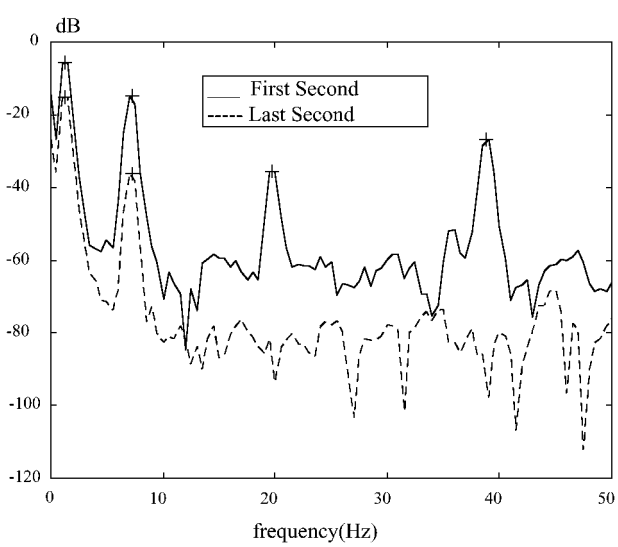

Fig. 3 PSD plots of free vibration of the beam.

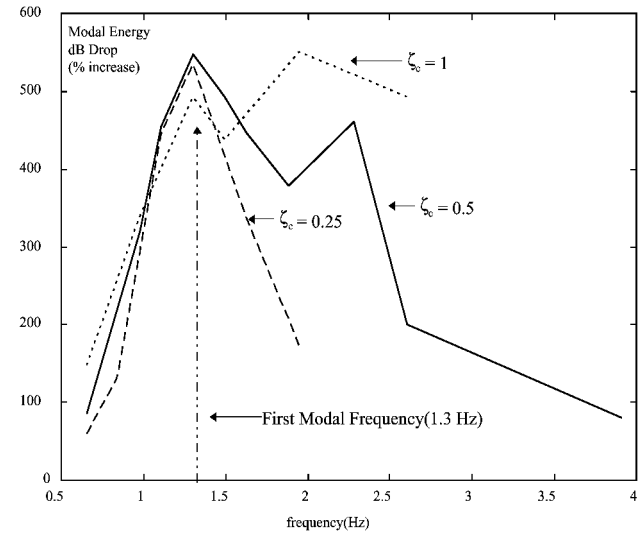

Fig. 4 Robustness results for different ζ_c.

The experimental results of suppression of first modal vibration using the PPF control are plotted in Fig. 4. In this figure the percentage values indicate percentage increase of the modal energy drop in decibels with PPF control as compared to that in the case of free vibration. It can be seen from this figure that the robustness increases as ζ_c is increased. This is as expected. The effectiveness of the PPF at the target frequency of 1.3 Hz was only slightly reduced when changing damping ratio from 0.25 to 1.0. This observation recommends using higher value of ζ_c in the PPF compensator design to achieve robustness because effectiveness at the targeted mode will not be much affected by a higher ζ_c. PPF control showed positive damping on all frequencies tested but dropped off rapidly when going below 75% of the targeted frequency or 200% above it. Overall, PPF control is robust to modal frequency variations. In addition, increased flexibility was not measurable even at 300% above the fundamental frequency. An optimal ζ_c for a given structure would depend on how accurate the modes are known and how much they would be expected to change, but a ζ_c of at least 0.5 should be chosen for robustness.

VI. Experimental Robustness Study of PPF in Multimode Vibration Suppression

PPF controls were tested for multimode vibration suppression. Two PPF filters are used. The first PPF filter targeted the first mode, and the second PPF filter targeted the second mode. The two PPF filters are in a parallel connection. Only actuator 1 along with the senor is used. Experiments were conducted to investigate the robustness of this type of controller. Table 3 shows the test results. In this table the percentage values indicate percentage increase of the modal energy drop in decibels with PPF control as compared to that in the case of free vibration. $\zeta_c = 0.5$ is used for both filters. For the first filter $G = 0.086$, and for the second filter $G = 0.003$. Both compensator frequencies are moved progressively higher than the targeted natural frequency. As seen from the table, the first mode damping falls off much quicker than the second mode. Part of the reason for this is the increased stiffness region of the first filter is moving closer to the second mode, thereby helping to increase the

Table 3 Robustness results for two PPF filter combination

PPF modal frequency, Hz	First mode decibel drop (% increase)	Second mode decibel drop (% increase)
$\omega_{c1} = 1.3 \times 1.0 = 1.3$ $\omega_{c2} = 7.1 \times 1.0 = 7.1$	58.33 (513%)	44.00 (97%)
$\omega_{c1} = 1.3 \times 1.25 = 1.625$ $\omega_{c2} = 7.1 \times 1.25 = 8.875$	42.16 (343%)	38.10 (70%)
$\omega_{c1} = 1.3 \times 1.5 = 1.95$ $\omega_{c2} = 7.1 \times 1.5 = 10.65$	36.14 (280%)	36.35 (62%)
$\omega_{c1} = 1.3 \times 1.75 = 2.275$ $\omega_{c2} = 7.1 \times 1.75 = 12.45$	30.11 (216%)	32.99 (47%)
$\omega_{c1} = 1.3 \times 2 = 2.6$ $\omega_{c2} = 7.1 \times 2 = 14.2$	17.88 (88%)	26.57 (19%)

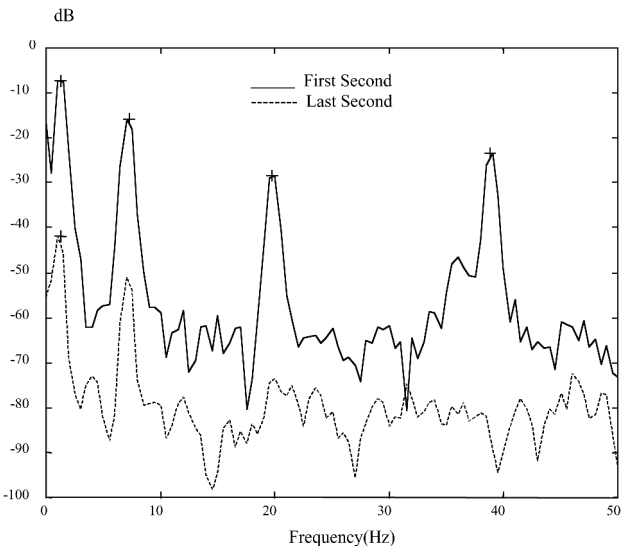

Fig. 5 PSD plot for two PPF filters (compensator frequencies are 1.5 times the targeted modal frequencies.).

damping effect. Just as in the single PPF case, the PPF combination shows good robustness for both modes. These results suggest that along with being robust the two PPF filter combination is effective in damping multiple modes over a range of frequencies. A PSD plot for the same controller graphically illustrating damping effectiveness is shown in Fig. 5.

VII. Conclusions

This research presents the experimental results robustness study of vibration suppression of a flexible structure using PPF control. The flexible structure is a cantilevered beam with PZT sensors and PZT actuators. PPF controls were implemented for single-mode vibration suppression and for multimode vibration suppression. Experiments found that PPF control is robust to frequency variations for single-mode and for multimode vibration suppressions.

Acknowledgments

The authors would like to thank A. Bronowicki and E. Rohleen, both of TRW, for their support in setting up Modular Control Patch.

References

[1]Goh, C. J., and Caughey, T. K., "On the Stability Problem Caused by Finited Actuator Dynamics in the Control of Large Space Structures," *International Journal of Control*, Vol. 41, No. 3, 1985, pp. 787–802.

[2]Balas, M. J., "Active Control of Flexible Systems," *Journal of Optimization Theory and Applications*, Vol. 25, No. 3, 1978, pp. 415–435.

[3]Friswell, M. I., and Inman, D., "The Relationship Between Positive Position Feedback and Output Feedback Controllers," *Journal of Smart Materials and Structures*, Vol. 8, No. 3, 1999, pp. 285–291.

[4]Fanson, J. L., and Caughey, T. K., "Positive Position Feedback Control for Large Space Structures," *AIAA Journal*, Vol. 28, No. 4, 1990, pp. 717–724.

[5]Bang, H., and Agrawal, B. N., "A Generalized Second Order Compensator Design for Vibration Control of Flexible Structures," 35th *AIAA/ASME/ASCE/AHS/ASC Structures, Structural Dynamics, and Materials Conference*, Part 5, AIAA, Washington, DC, 1994, pp. 2438–2448.

[6]Sciulli, D., and Inman, D. J., "Isolation Design for a Flexible System," *Journal of Sound and Vibration*, Vol. 216, No. 2, 1998, pp. 251–267.

[7]Denoyer, K. K., and Kwak, M. K., "Dynamic Modeling and Vibration Suppression of a Swelling Structure Utilizing Piezoelectric Sensors and Actuators," *Journal of Sound and Vibration*, Vol. 189, No. 1, 1996, pp. 13–31.

[8]Meyer, J. L., Harrington, W. B., Agrawal, B. N., and Song, G., "Vibration Suppression of a Spacecraft Flexible Appendage Using Smart Material," *Journal of Smart Materials and Structures*, Vol. 7, No. 1, 1998, pp. 95–104.

[9]Song, G., Schmidt, S. P., and Agrawal, B. N., "Active Vibration Suppression of a Flexible Structure Using Smart Material and Modular Control Patch," *Journal of Aerospace Engineering*, Vol. 214, No. G4, 2000, pp. 217–229.

Approximate Equations for the Coplanar Restricted Three-Body Problem

Mayer Humi*
Worcester Polytechnic Institute, Worcester, Massachusetts 01609

Introduction

THE fuel-optimal rendezvous problem for a spacecraft with a satellite in a central force field has been the subject of several papers [1–6] in the last decade. In this Note we address the rendezvous problem of a spacecraft with a moon, comet, or asteroid (whose gravitational field is not negligible) in the central force field of a (large) third body. In this setting we derive reduced equations for the motion of the spacecraft in the vicinity of the smaller body (moon) in three dimensions. We present a generalization, under some restrictions, to the Jacobi integral.[7]

Clearly the problem we consider here is closely related to the restricted three-body problem in two dimensions,[7,8] which deals with the motion of a body of negligible mass in the gravitational field of two other celestial bodies. However in this setting all three bodies are assumed to remain always in one plane.

To put our results in proper perspective, we note that Edelbaum[9] made one of the first attempts to address the rendezvous problem between a spacecraft and a satellite in a near circular orbit. A simpler model was derived by Clohessy and Wiltshire,[10] whose equations can be found now in books on orbital mechanics.[4] Carter and Humi,[1] Humi,[2] and Carter and Brient[3] found some analytical solutions for the rendezvous problem when the satellite is in a general Keplerian orbit and derived a generalization[2] of these equations in the presence of a general central force field. Currently an effort is under way to include the effect of drag (linear and quadratic) in the rendezvous equations.[6] (For a more extensive list of contributions to the rendezvous problem, see the reference lists in Refs. 1 and 6).

Derivation of the Reduced Equations

In an inertial coordinate system whose origin is at the center of the central body E, we let $\boldsymbol{R}$, $\boldsymbol{\rho}$ denote the position of the moon and the spacecraft, respectively, and $\boldsymbol{r}$ the relative position of the

Received 12 December 2000; revision received 11 June 2001; accepted for publication 22 August 2001.

*Professor of Mathematics, Department of Mathematical Sciences; mhumi@wpi.edu.